

Magnetic Properties of Reactive Co-Sputtered NiFe-Oxide Samples

AQ:1 Bi  D. C.  ¹, Andres A. Oliva¹, Anival Ayala², Shankar Acharya  ¹, Fidele Twagirayezu¹, James Nick Talbert¹, Luisa M. Scolfaro¹, and Wilhelmus J. Geerts¹

AQ:2 ¹Department of Physics, Texas State University, San Marcos, TX 78666 USA

²MSEC, Texas State University, San Marcos, TX 78666 USA

In this paper, we discuss the properties of reactive radio-frequency-sputtered Fe-doped NiO thin films co-sputtered at different oxygen flow rates. The films were deposited in an AJA Orion sputtering system from metallic NiFe-19 at.% targets. The deposition rate was monitored before and after deposition using a quartz crystal monitor. The deposition rate at the sample location depends strongly on the O₂ flow. At lower oxygen flows, the deposition rate increases with oxygen flow caused by the oxidation of the sample. At higher oxygen flow rates, the deposition rate decreases with increasing oxygen flow. This is caused by poisoning of the targets resulting in a lower deposition rate. The oxygen content of the samples increases with the oxygen flow rate. This conclusion is supported by vibrating sample magnetometer measurements that show an increase in the magnetic moment for films sputtered at lower O₂ flows. To determine the chemical state of the elements, the X-ray photoelectron spectroscopy (XPS) analysis of the samples was carried out ex situ on films capped with a Pt or Au layer. Prior to the XPS measurements, part of the cap layers but not all were removed with an Ar sputtering gun in the XPS chamber. The XPS results show that the ratio of the Ni⁰-Ni²⁺ atoms in the film decreases with the oxygen flow. The Fe-XPS spectra of the films sputtered at different oxygen flows look very similar to each other but different from XPS studies done on oxidized permalloy by others showing that RF-sputtered NiFe-oxide is different from oxidized permalloy. The comparison of the XPS data for the samples sputtered at 20 sccm covered with Pt cap and Au cap was also done and shows smaller metallic Ni peaks for the sample capped with Au than samples capped with Pt, possibly caused by partly sputtering through the cap layer for the Pt-capped samples influencing the stoichiometry of the top layer of the NiFe-oxide.

Index Terms—Magnetism, thin films, vibrating sample magnetometer (VSM), X-ray photoelectron spectroscopy (XPS).

I. INTRODUCTION

NiO thin films and its doped cousins have been extensively studied for a large variety of applications, including solar cells, novel batteries, resistive nonvolatile random access memory (RRAM), spintronic electronics, catalyzers, and gas sensors. Its applicability originates from the ability to modify its properties by changing the ratio of O to metal atoms and to modify its crystallinity by doping with other transition metals [1].

Here, we discuss the properties of reactive radio-frequency co-sputtered NiO and Fe-doped NiO thin films sputtered at the low oxygen flow rate and focus on the magnetic and chemical properties. This is relevant for the application of these films in RRAM devices. NiO and NiFeO RRAM devices are based on reversible switching between a high-resistance semiconducting state and a low-resistance metallic state. In the low-resistance state, metallic filaments are formed between the top and bottom electrodes at one or more locations in the device. The distribution of the filaments is normally determined by removing the top electrode and performing conductive AFM studies of the oxide surface to find the location and the size of the filaments. This type of study is destructive. Better switching studies could be performed if the location and size of the filaments could be detected without removing the top electrode.

Manuscript received June 6, 2018; revised August 6, 2018; accepted August 13, 2018. Corresponding author: W. J. Geerts (e-mail: wjgeerts@txstate.edu).

Color versions of one or more of the figures in this paper are available online at <http://ieeexplore.ieee.org>.

Digital Object Identifier 10.1109/TMAG.2018.2866788

The magnetic signature of low oxygen concentration NiO and NiFeO in combination with the magnetic force microscopy can provide a method. This is the first report on such a study. The work supplements data obtained on NiO and NiFeO thin films sputtered at much larger oxygen flow rates [2].

II. EXPERIMENTAL PROCEDURE

A. Sample Preparation

The samples were deposited in an  Orion sputtering system that is capable of depositing metal and dielectric films on substrates up to 4 in in diameter. The system is equipped with five AJA high-vacuum magnetron sputtering sources that are powered by RF generators (300 W) or dc generators (500 W) for single, multi-layer, or co-deposition. The system utilizes a motorized, rotating substrate holder to achieve excellent uniformity, allows the co-deposition of alloy films, and facilitates the deposition of clean, thin-film multilayers [3]. The permalloy oxide (PyO) thin films reported on in this paper were deposited from metallic permalloy targets by reactive RF magnetron sputtering using two guns, which are located on the opposite sides of the chamber. The angle they make with the normal of the substrate holder is 107°. To further improve the homogeneity of the films, the substrate holder was rotated during deposition. Films were deposited on glass microscope slides and Si wafers covered with a 2 nm thick native SiO₂ layer. All the films were deposited at room temperature. Prior to deposition, the substrates were sequentially rinsed in water, acetone, and methanol. Each next solvent was used to rinse the preceding solvent of the wafer. The last cleaning step was

69 done on a spinner with isopropyl alcohol. The chamber was
70 pumped down to a base pressure of $<4 \times 10^{-7}$ torr by a
71 roughing and a turbo pump. Two similar RF sources at a power
72 of 200 W each were used. The flow of gas was controlled by
73 an MKS mass flow controller (Ar) and an MKS mass flow
74 meter (O_2). The total flow was kept at 50 sccm resulting
75 in a sputter pressure of approximately 8 mtorr. The oxygen
76 flow was kept constant during deposition. After opening the
77 shutters mounted on the chimneys of the guns, the targets
78 were pre-sputtered for 1 min before the deposition rate was
79 measured with the quartz crystal monitor (QCM) mounted
80 to the back of the substrate shutter. The accumulated film
81 thickness was measured with the QCM over a period of 50 s
82 prior to opening the substrate shutter, and the deposition rate
83 was calculated from this accumulated thickness. The total
84 deposition time for each sample was kept at 1200 s. During
85 deposition, the substrate was rotated at 30 r/min. Deposition
86 was done at room temperature. This method has been shown
87 to produce high-quality polycrystalline films. The thickness
88 of the thin-film samples was verified by ellipsometry. The
89 deposition rates calculated from the ellipsometry thickness and
90 the deposition time were similar to the rate measured with the
91 QCM. The films sputtered at low oxygen flow had a typical
92 thickness of around 140 nm, while the films sputtered at
93 20 sccm were much thinner (17 nm). All samples were covered
94 with a 5 nm thick Au or Pt cap layer to avoid oxidation when
95 taken out of the sputtering system. This layer was sputtered
96 with a dc magnetron sputter gun at 50 W and 30 sccm Ar flow.

97 B. Magnetic Measurement Procedure

98 The magnetic moment of the films was measured by a
99 vibrating sample magnetometer (VSM) from Quantum Design.
100 The sample was vibrated in an external magnetic field
101 at 40 Hz. A pickup coil set is placed around the sample. When
102 the sample is moved, the total magnetic field passing through
103 the pickup coils fluctuates, and this magnetic flux induces a
104 proportional induction current in the coil set, which can be
105 measured. An induced current is proportional to the sample's
106 magnetic moment. The fused quartz sample holder itself does
107 hardly contribute to the signal as it extends above and below
108 the pickup coils. Its vibrations hardly cause a flux change
109 through the set of pickup coils [4]–[6].

110 As NiO and NiFeO are antiferromagnetic materials, a large
111 magnetic moment is not expected. Defects and the surface
112 of the films, however, can have a significant magnetic signal.
113 In particular, the samples made at lower oxygen flows could
114 have a significant magnetic moment originating from oxygen
115 vacancy clusters. As the expected moment of the films is small,
116 a special technique is used to suppress the magnetic signature
117 of the substrate which can be much larger than the thin film.
118 Two techniques are employed [2].

- 119 1) A silicon wafer was used as a substrate because of the
120 low magnetic moment of silicon (slightly diamagnetic)
121 and the availability of thin wafers.
- 122 2) Bare silicon tiles were mounted above and below the
123 sample on the VSM sample holder to suppress the
124 magnetic signal of the diamagnetic silicon substrate.

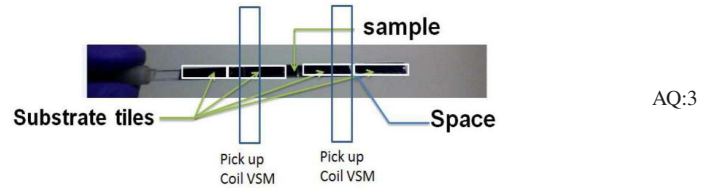


Fig. 1. Magnetic measurement configuration.

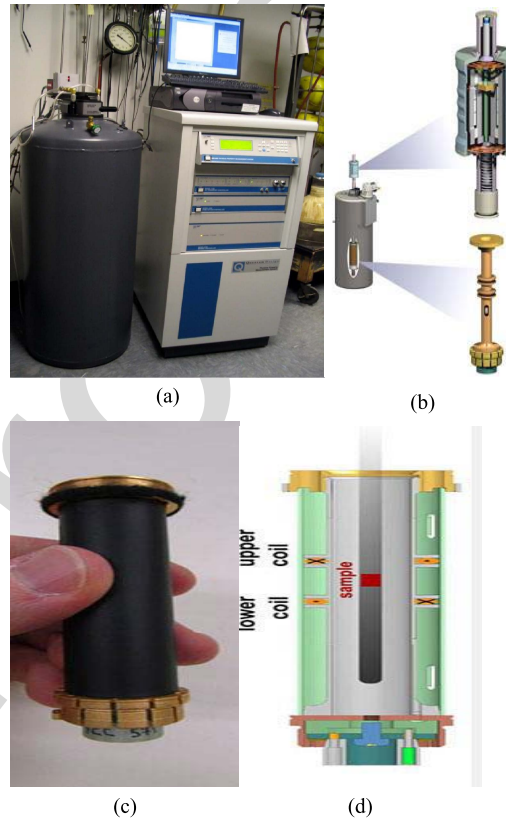


Fig. 2. (a) PPMS apparatus. (b) VSM attachments for PPMS. (c) Photograph of the VSM puck. (d) Cross section of VSM puck.

A physical property measurement system (PPMS) with VSM attachments [Fig. 2(a) and (b)] was used to measure the magnetic moment in the NiFeO sample prepared at the AJA sputtering system in the clean room of Texas State University. The PPMS system and VSM attachments are shown as follows. The pickup coils for this apparatus are in the VSM puck [Fig. 2(c) and (d)], which is inserted into the PPMS. This system may measure fields ranging from +9 to -9 T and can measure temperatures ranging from 4 to 300 K. For these measurements, the field was changed at a rate of 180 Oe/s, and measurements were done at 4 K and at room temperatures.

137 C. XPS Measurement Procedure

X-ray photoelectron spectroscopy (XPS) measurements were made using an XPS PHI Quantum 2000 Scanning ESCA microprobe. The chamber contains an Al $\text{K}\alpha$ X-ray source in which incoming X-rays are parallel to the surface normal. The system allows for measurements with an analysis resolution of about 1 eV [5]. The beam power was 50 W and

125 AQ:4
126
127
128
129
130
131
132
133
134
135
136

137
138
139
140
141
142
143

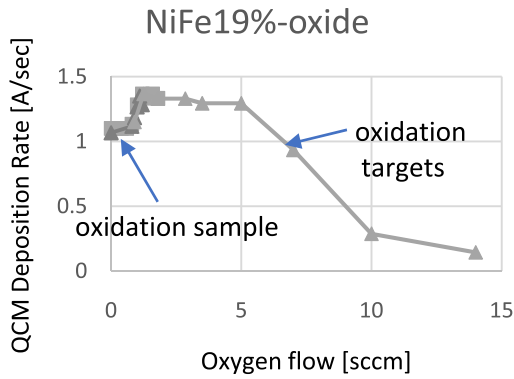


Fig. 3. Deposition rate as a function of the oxygen flow for NiFe-19% co-sputtering at 200 W.

144 the takeoff angle was 45° . The X-ray spot size was $200\ \mu\text{m}$
 145 and the analysis was done on an area of $500\ \mu\text{m} \times 500\ \mu\text{m}$. Under these conditions, the information depth is approximately
 146 10 nm. Prior to the scans, part of the Pt or Au cap layer
 147 was removed by argon sputtering. To avoid the effects of
 148 preferential sputtering on the NiFe-oxide XPS spectra, part of
 149 the cap layers were kept in place. As Au has a larger sputter
 150 rate, the samples with an Au cap layer were sputtered for only
 151 1 min while the samples covered with a Pt cap layer were
 152 sputtered for 3 min. The pass energies were 187 eV for the
 153 survey and 58 eV for the high-resolution scans. All energies
 154 are referenced with respect to the main C peak at 284.8 eV.
 155

156 III. EXPERIMENTAL RESULTS

157 Fig. 3 shows the measured deposition rate as a function
 158 of the oxygen flow for our process. The deposition shows a
 159 maximum as the function of the oxygen flow. At lower oxygen
 160 flow rates, the deposition rate increases with the oxygen flow.
 161 We believe that this increase (24%) is due to the introduction
 162 of oxygen into the system resulting in the oxidation of the
 163 freshly deposited film. As for a fully oxidized film one would
 164 expect an increase in 27%, the films sputtered at low oxygen
 165 flow are not stoichiometric but contain a significant amount
 166 of oxygen vacancies. At higher oxygen flow, i.e., above
 167 5 sccm, the deposition rate decreases strongly. We believe
 168 that this is caused by the oxidation of the targets. This is
 169 often referred to as poisoning of the target [8]. It is well
 170 known that NiFe-oxide has a much lower sputter rate than
 171 metallic permalloy. Although the oxidation of the targets also
 172 takes place at lower oxygen flow rates, at those low oxygen
 173 flow rates, the removal rate of the material from the targets
 174 is much higher than the rate with which an oxide layer is
 175 formed on the target. Therefore, below 5 sccm, the target
 176 surfaces are clean of oxide and most of the sputtered material
 177 is metallic permalloy. From 5 sccm and above, the removal
 178 of the material from the targets can no longer keep up with
 179 the oxidation and the deposition rate collapses. Note that for
 180 our process, the QCM deposition rate is significantly lower
 181 than the rate with which the material is removed from the
 182 targets. The short mean free path of the sputtered atoms at
 183 8 mtorr results in a diverging atom beam that has a diameter
 184 significantly larger than the target diameter at the location

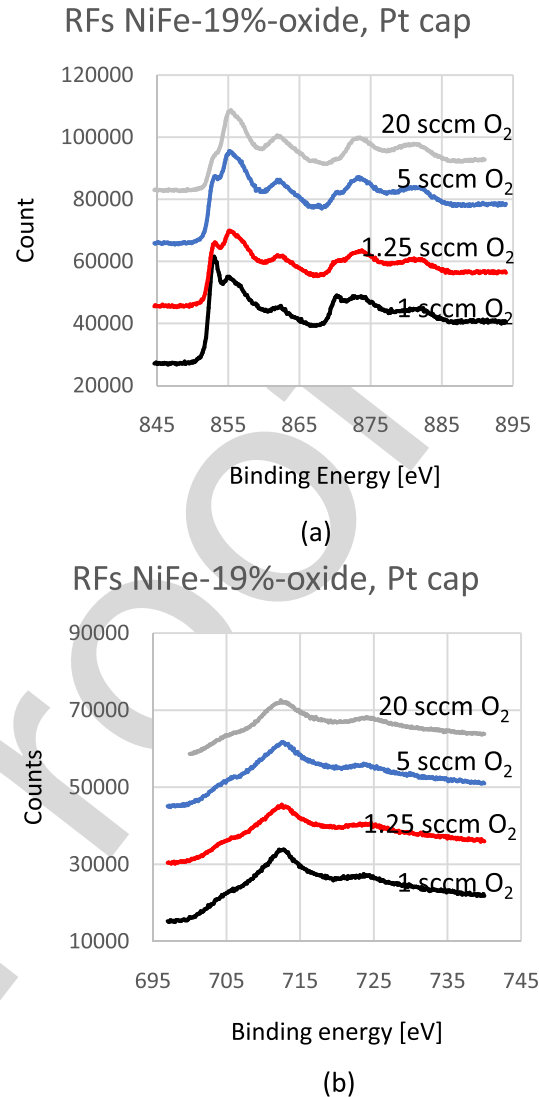


Fig. 4. XPS spectra of RF-sputtered NiFe-oxide samples sputtered at different oxygen flow rates covered with the Pt cap layer. (a) Ni spectrum. (b) Fe spectrum. Spectra are shifted in the y-direction to reveal the detail.

185 of the substrate. From the measurements of the deposition
 186 rate versus the substrate distance, we expect at least a factor
 187 10 difference between the QCM rate at our substrate position
 188 and the target material removal rate. Fig. 4 shows the XPS
 189 spectrum of $\text{Ni}(2\text{p}_{3/2})$ and $\text{Fe}(2\text{p})$ of samples sputtered at
 190 various oxygen flow rates. This is the XPS data obtained from
 191 the samples that had a Pt cap layer. Note that the ratio of the
 192 Ni^0 to Ni^{2+} decreases with oxygen flow, but the Ni^0 peak is
 193 still visible in the Ni-spectrum for films sputtered at 20 sccm
 194 oxygen flow. The Fe-XPS spectra of the films sputtered at
 195 a different oxygen flow look very similar to each other
 196 (see Fig. 4). Our Fe spectra differ though from the XPS spectra
 197 of oxidized Permalloy films published in [9], which show a
 198 steep slope at 700 eV while all our films show a very gradual
 199 slope. The absence of a distinct Fe^0 peak suggests that most
 200 Fe is oxidized, and oxygen vacancies prefer to reside next
 201 to nickel atoms. Since the resistivity of the films sputtered at
 202 20 sccm O_2 is much lower than the films sputtered at 5 sccm, we
 203 believe that the films sputtered at 20 sccm oxygen

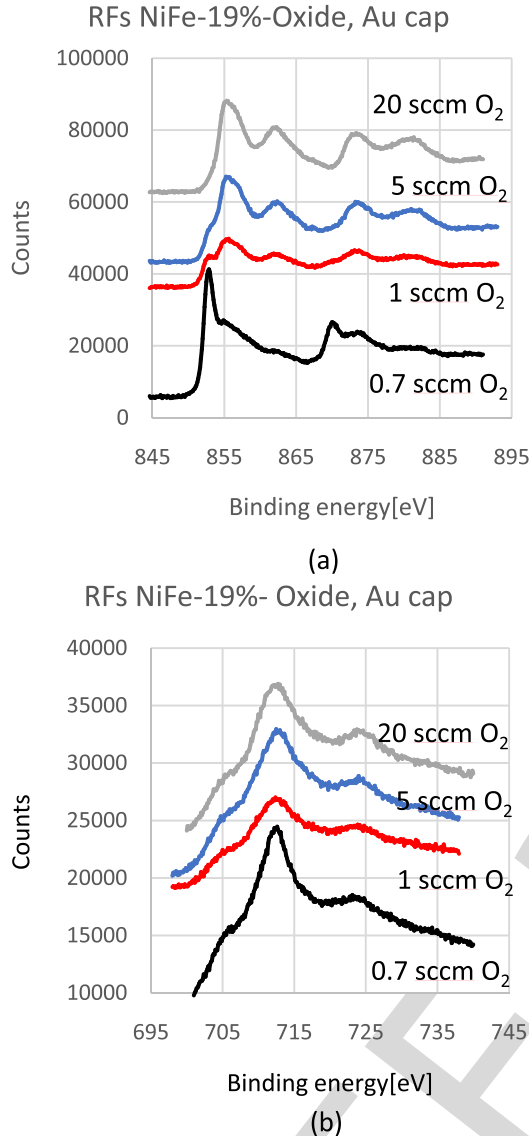


Fig. 5. XPS spectra of RF-sputtered NiFe-oxide samples sputtered at different oxygen flow rates covered with the Au cap layer. (a) Ni spectrum. (b) Fe spectrum. Spectra are shifted in the y-direction to reveal the detail.

flow contain metal vacancies. However, no Ni³⁺ peak was observed in our NiFe-oxide films [10]. The interpretation of the Fe-XPS spectrum is challenging as for Al $\text{k}\alpha$ radiation an Auger Ni-peak is present in the middle of the Fe-XPS spectrum, i.e., 712 eV. In addition, Pt has a peak in the Fe-XPS spectrum at 725 eV near the position of a metallic Fe peak. The XPS data for the samples covered with an Au cap layer are shown in Fig. 5. Note that the counts of the Au-capped samples of Fig. 5 are significantly lower than those of the Pt capped layers of Fig. 4. This suggests that the remaining Au cap layer in the samples of Fig. 5 is thicker than the remaining Pt cap layer in the samples of Fig. 4. A detailed analysis of the data of Figs. 4 and 5 using a rough estimate of the sputter rates of Au and Pt suggests that we might have sputtered through part of the Pt layer for the results shown in Fig. 4 and that the ratio of the Ni⁰ to Ni²⁺ oxygen peaks in Fig. 4 was affected by a preferential sputtering of oxygen of part of the NiFeO films of Fig. 4. The Fe spectra of Fig. 5 are similar to the

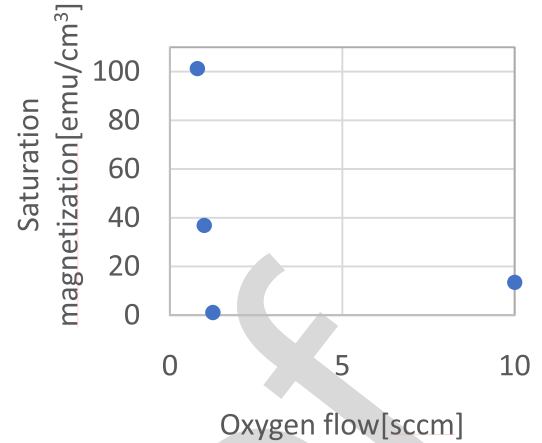


Fig. 6. Variation of saturation magnetization with oxygen concentration for different films.

Fe spectra of Fig. 4. It might not be possible to distinguish the metallic Fe-XPS peak at 707 eV from the Ni Auger peak at 712 eV. An additional XPS analysis was done in another system using Mg $\text{k}\alpha$ radiation on uncapped layers. For an Mg source, the nickel Auger peaks shift outside the Fe spectrum. The same gradual slope in the XPS Fe spectrum near 700 eV was observed for those experiments. Therefore, the gradual slope observed in the Fe spectrum might be characteristic for reactive RF-sputtered PyO films. It is definitely not caused by the cap layer and does not depend on the X-ray source, so is unlikely due to the Auger peak of nickel.

Fig. 6 shows the measured magnetic moment per unit volume as a function of the oxygen flow. A decrease in the saturation magnetization is observed for higher oxygen flows. This might be due to a more fully oxidation of the films sputtered at high oxygen flow. Note that NiFe-oxide was shown to have a rock salt crystal structure [11], [12] and discrete Fourier transform calculations have shown that it is antiferromagnetic [13]. A sharp decrease in the magnetic moment was observed when the oxygen flow was increased to 1.25 sccm. For films deposited at flows above 1.25 sccm, the saturation magnetization slightly increases similar to what was observed by Twagirayezu on RF-sputtered films using a single source [2].

IV. CONCLUSION

The deposition rate of reactive RF-sputtered NiFeO and NiO films depends on the oxygen flow rate during deposition. For low oxygen flows (below 1.25 sccm O₂), the deposition rate increases with increased oxygen flow. This is caused by the oxidation of the deposited metal film. This is consistent by magnetic measurements that show an increase in the magnetic moment for films sputtered at lower O₂ flows. At moderate oxygen flows, i.e., between 1.25 and 5 sccm, the deposition rate is constant. At high oxygen flow (above 5 sccm), the deposition rate sharply decreases. At these flows, the sputtering of the material of the target can no longer keep up with its oxidation and poisoning of the target takes place. The XPS analysis showed that the ratio of the Ni⁰ to Ni²⁺ decreases with oxygen flow. The XPS results also

suggest that sputtering NiFe-oxide with argon leads to the preferential sputtering of oxygen (a reduction of NiFeO) for oxygen-rich compositions. The XPS Fe spectra of the films sputtered at a different oxygen flow look very similar to each other but different from Fe-XPS spectra measured on oxidized permalloy samples by others. A distinct metallic Fe peak was lacking in the Fe spectra, which suggests that oxygen vacancies in NiFe-oxide prefer nickel neighbors and most of the Fe atoms are oxidized. The observed increase in the magnetic moment with oxygen vacancy concentration could provide a method to magnetically detect the location and distribution of low oxygen concentration filaments in RRAM devices. Such method is in need of systematic switching studies to further the development of the RRAM technology.

ACKNOWLEDGMENT

This work was supported in part by a DOD Grant (HBCU/MI) under Grant W911NF-15-1-0394 and in part by NSF through a DMR-MRI Grant under Award 1726970. The authors would like to thank the staff of the nanofabrication fab at Texas State for their support, particularly A. Sherrow and Dr. C. Smith. They would also like to thank Dr. T. Hossain and A. Ghatak-Roy for their help with the XPS measurements.

REFERENCES

[1] I. Hotovy, J. Huran, L. Spiess, S. Hascik, and V. Rehacek, "Preparation of nickel oxide thin films for gas sensors applications," *Sens. Actuators B, Chem.*, vol. 57, pp. 147–152, Sep. 1999.

[2] F. Twagirayezu, M. A. AhadTalukder, and W. J. Geerts, "Magnetic properties of RF sputtered NiO and Ni_{0.8}Fe_{0.2}O₁-samples grown on SiO₂/Si substrates," *Mater. Res. Innov.*, Jul. 2018.

[3] AJA International Incorporated. [Online]. Available: <http://www.jaint.com/atac-orion-series>

[4] J. Hack, M. H. Ludwig, W. Geerts, and R. E. Hummel, "Advances in micro-crystalline and nano-crystalline semiconductors," vol. 452, p. 147, 1997.

[5] E. O. Samwel, T. Bolhuis, and J. C. Lodder, "An alternative approach to vector vibrating sample magnetometer detection coil setup," *Rev. Sci. Instrum.*, vol. 69, no. 9, p. 3204, 1998.

[6] S. Thota, J. H. Shim, and M. S. Seehra, "Size-dependent shifts of the Néel temperature and optical band-gap in NiO nanoparticles," *J. Appl. Phys.*, vol. 114, no. 21, p. 214307, 2013.

[7] D. Wanger *et al.*, *Handbook of X-Ray Photoelectron Spectroscopy*. 1997.

[8] N. R. Murphy, L. Sun, J. T. Grant, J. G. Jones, and R. Jakubiak, "Molybdenum oxides deposited by modulated pulse power magnetron sputtering: Stoichiometry as a function of process parameters," *J. Electron. Mater.*, vol. 44, pp. 3677–3686, Oct. 2015.

[9] M. Salou, B. Lescop, S. Rioual, A. Lebon, J. Ben Youssef, and B. Rouvelliou, "Initial oxidation of polycrystalline Permalloy surface," *Surf. Sci.*, vol. 602, pp. 2901–2906, Sep. 2008.

[10] S. Uhlenbrock, C. Scharfschwerdt, M. Neumann, G. Illing, and H.-J. Freund, "The influence of defects on the Ni₂p and O 1s XPS of NiO," *J. Phys., Condens. Matter*, vol. 4, no. 40, pp. 7973–7978, 1992.

[11] M. A. A. Talukder, Y. Cui, M. Compton, W. Geerts, L. Scolfaro, and S. Zollner, "FTIR ellipsometry study on RF sputtered permalloy-oxide thin films," *MRS Adv.*, vol. 1, no. 49, pp. 3361–3366, 2016.

[12] A. K. Bandyopadhyay, S. E. Rios, A. Tijerina, and C. J. Gutierrez, "The influence of ion beam sputtering geometry on metastable (Ni₈₁Fe₁₉)O/Ni₈₁Fe₁₉ exchange biased bilayers," *J. Alloys Compounds*, vol. 369, pp. 217–221, Apr. 2004.

[13] J. E. Petersen, F. Twagirayezu, L. M. Scolfaro, P. D. Borges, and W. J. Geerts, "Electronic and optical properties of antiferromagnetic iron doped NiO—A first principles study," *AIP Adv.*, vol. 7, no. 5, p. 055711, 2017.

AUTHOR QUERIES

AUTHOR PLEASE ANSWER ALL QUERIES

PLEASE NOTE: We cannot accept new source files as corrections for your paper. If possible, please annotate the PDF proof we have sent you with your corrections and upload it via the Author Gateway. Alternatively, you may send us your corrections in list format. You may also upload revised graphics via the Author Gateway.

AQ:1 = Please confirm whether the author name “Binod D. C.” is correct as set.

AQ:2 = Please provide expansions for MSEC, AJA, MKS, and ESCA.

AQ:3 = Please provide in-text citations for Fig. 1.

AQ:4 = Please check and confirm whether the citation for Fig. 2 provided in the sentence “A physical property measurement system (PPMS)...” is correct.

AQ:5 = Author: Please confirm or add details for any funding or financial support for the research of this article.

AQ:6 = Please confirm author names, article title, and journal title for ref. [2]. Also provide the volume no., and page range.

AQ:7 = Please provide the accessed date for ref. [3].

AQ:8 = Please confirm the author names, and title for ref. [4]. Also provide the journal title.

AQ:9 = Please provide the publisher name and publisher location for ref. [7].

Magnetic Properties of Reactive Co-Sputtered NiFe-Oxide Samples

AQ:1 Binod D. C.^{✉1}, Andres A. Oliva¹, Anival Ayala², Shankar Acharya^{✉1}, Fidele Twagirayezu¹,
James Nick Talbert¹, Luisa M. Scolfaro¹, and Wilhelmus J. Geerts¹

AQ:2 ¹Department of Physics, Texas State University, San Marcos, TX 78666 USA

²MSEC, Texas State University, San Marcos, TX 78666 USA

In this paper, we discuss the properties of reactive radio-frequency-sputtered Fe-doped NiO thin films co-sputtered at different oxygen flow rates. The films were deposited in an AJA Orion sputtering system from metallic NiFe-19 at.% targets. The deposition rate was monitored before and after deposition using a quartz crystal monitor. The deposition rate at the sample location depends strongly on the O₂ flow. At lower oxygen flows, the deposition rate increases with oxygen flow caused by the oxidation of the sample. At higher oxygen flow rates, the deposition rate decreases with increasing oxygen flow. This is caused by poisoning of the targets resulting in a lower deposition rate. The oxygen content of the samples increases with the oxygen flow rate. This conclusion is supported by vibrating sample magnetometer measurements that show an increase in the magnetic moment for films sputtered at lower O₂ flows. To determine the chemical state of the elements, the X-ray photoelectron spectroscopy (XPS) analysis of the samples was carried out ex situ on films capped with a Pt or Au layer. Prior to the XPS measurements, part of the cap layers but not all were removed with an Ar sputtering gun in the XPS chamber. The XPS results show that the ratio of the Ni⁰-Ni²⁺ atoms in the film decreases with the oxygen flow. The Fe-XPS spectra of the films sputtered at different oxygen flows look very similar to each other but different from XPS studies done on oxidized permalloy by others showing that RF-sputtered NiFe-oxide is different from oxidized permalloy. The comparison of the XPS data for the samples sputtered at 20 sccm covered with Pt cap and Au cap was also done and shows smaller metallic Ni peaks for the sample capped with Au than samples capped with Pt, possibly caused by partly sputtering through the cap layer for the Pt-capped samples influencing the stoichiometry of the top layer of the NiFe-oxide.

Index Terms—Magnetism, thin films, vibrating sample magnetometer (VSM), X-ray photoelectron spectroscopy (XPS).

I. INTRODUCTION

NiO thin films and its doped cousins have been extensively studied for a large variety of applications, including solar cells, novel batteries, resistive nonvolatile random access memory (RRAM), spintronic electronics, catalyzers, and gas sensors. Its applicability originates from the ability to modify its properties by changing the ratio of O to metal atoms and to modify its crystallinity by doping with other transition metals [1].

Here, we discuss the properties of reactive radio-frequency co-sputtered NiO and Fe-doped NiO thin films sputtered at the low oxygen flow rate and focus on the magnetic and chemical properties. This is relevant for the application of these films in RRAM devices. NiO and NiFeO RRAM devices are based on reversible switching between a high-resistance semiconducting state and a low-resistance metallic state. In the low-resistance state, metallic filaments are formed between the top and bottom electrodes at one or more locations in the device. The distribution of the filaments is normally determined by removing the top electrode and performing conductive AFM studies of the oxide surface to find the location and the size of the filaments. This type of study is destructive. Better switching studies could be performed if the location and size of the filaments could be detected without removing the top electrode.

Manuscript received June 6, 2018; revised August 6, 2018; accepted August 13, 2018. Corresponding author: W. J. Geerts (e-mail: wjgeerts@txstate.edu).

Color versions of one or more of the figures in this paper are available online at <http://ieeexplore.ieee.org>.

Digital Object Identifier 10.1109/TMAG.2018.2866788

The magnetic signature of low oxygen concentration NiO and NiFeO in combination with the magnetic force microscopy can provide a method. This is the first report on such a study. The work supplements data obtained on NiO and NiFeO thin films sputtered at much larger oxygen flow rates [2].

II. EXPERIMENTAL PROCEDURE

A. Sample Preparation

The samples were deposited in an AJA Orion sputtering system that is capable of depositing metal and dielectric films on substrates up to 4 in in diameter. The system is equipped with five AJA high-vacuum magnetron sputtering sources that are powered by RF generators (300 W) or dc generators (500 W) for single, multi-layer, or co-deposition. The system utilizes a motorized, rotating substrate holder to achieve excellent uniformity, allows the co-deposition of alloy films, and facilitates the deposition of clean, thin-film multilayers [3]. The permalloy oxide (PyO) thin films reported on in this paper were deposited from metallic permalloy targets by reactive RF magnetron sputtering using two guns, which are located on the opposite sides of the chamber. The angle they make with the normal of the substrate holder is 107°. To further improve the homogeneity of the films, the substrate holder was rotated during deposition. Films were deposited on glass microscope slides and Si wafers covered with a 2 nm thick native SiO₂ layer. All the films were deposited at room temperature. Prior to deposition, the substrates were sequentially rinsed in water, acetone, and methanol. Each next solvent was used to rinse the preceding solvent of the wafer. The last cleaning step was

69 done on a spinner with isopropyl alcohol. The chamber was
70 pumped down to a base pressure of $<4 \times 10^{-7}$ torr by a
71 roughing and a turbo pump. Two similar RF sources at a power
72 of 200 W each were used. The flow of gas was controlled by
73 an MKS mass flow controller (Ar) and an MKS mass flow
74 meter (O_2). The total flow was kept at 50 sccm resulting
75 in a sputter pressure of approximately 8 mtorr. The oxygen
76 flow was kept constant during deposition. After opening the
77 shutters mounted on the chimneys of the guns, the targets
78 were pre-sputtered for 1 min before the deposition rate was
79 measured with the quartz crystal monitor (QCM) mounted
80 to the back of the substrate shutter. The accumulated film
81 thickness was measured with the QCM over a period of 50 s
82 prior to opening the substrate shutter, and the deposition rate
83 was calculated from this accumulated thickness. The total
84 deposition time for each sample was kept at 1200 s. During
85 deposition, the substrate was rotated at 30 r/min. Deposition
86 was done at room temperature. This method has been shown
87 to produce high-quality polycrystalline films. The thickness
88 of the thin-film samples was verified by ellipsometry. The
89 deposition rates calculated from the ellipsometry thickness and
90 the deposition time were similar to the rate measured with the
91 QCM. The films sputtered at low oxygen flow had a typical
92 thickness of around 140 nm, while the films sputtered at
93 20 sccm were much thinner (17 nm). All samples were covered
94 with a 5 nm thick Au or Pt cap layer to avoid oxidation when
95 taken out of the sputtering system. This layer was sputtered
96 with a dc magnetron sputter gun at 50 W and 30 sccm Ar flow.

97 B. Magnetic Measurement Procedure

98 The magnetic moment of the films was measured by a
99 vibrating sample magnetometer (VSM) from Quantum Design.
100 The sample was vibrated in an external magnetic field
101 at 40 Hz. A pickup coil set is placed around the sample. When
102 the sample is moved, the total magnetic field passing through
103 the pickup coils fluctuates, and this magnetic flux induces a
104 proportional induction current in the coil set, which can be
105 measured. An induced current is proportional to the sample's
106 magnetic moment. The fused quartz sample holder itself does
107 hardly contribute to the signal as it extends above and below
108 the pickup coils. Its vibrations hardly cause a flux change
109 through the set of pickup coils [4]–[6].

110 As NiO and NiFeO are antiferromagnetic materials, a large
111 magnetic moment is not expected. Defects and the surface
112 of the films, however, can have a significant magnetic signal.
113 In particular, the samples made at lower oxygen flows could
114 have a significant magnetic moment originating from oxygen
115 vacancy clusters. As the expected moment of the films is small,
116 a special technique is used to suppress the magnetic signature
117 of the substrate which can be much larger than the thin film.
118 Two techniques are employed [2].

- 119 1) A silicon wafer was used as a substrate because of the
120 low magnetic moment of silicon (slightly diamagnetic)
121 and the availability of thin wafers.
- 122 2) Bare silicon tiles were mounted above and below the
123 sample on the VSM sample holder to suppress the
124 magnetic signal of the diamagnetic silicon substrate.

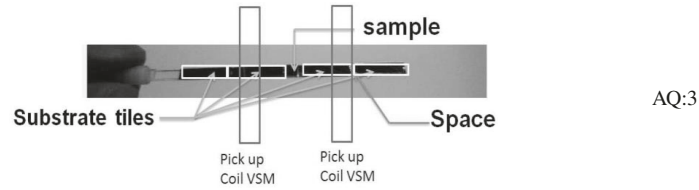


Fig. 1. Magnetic measurement configuration.

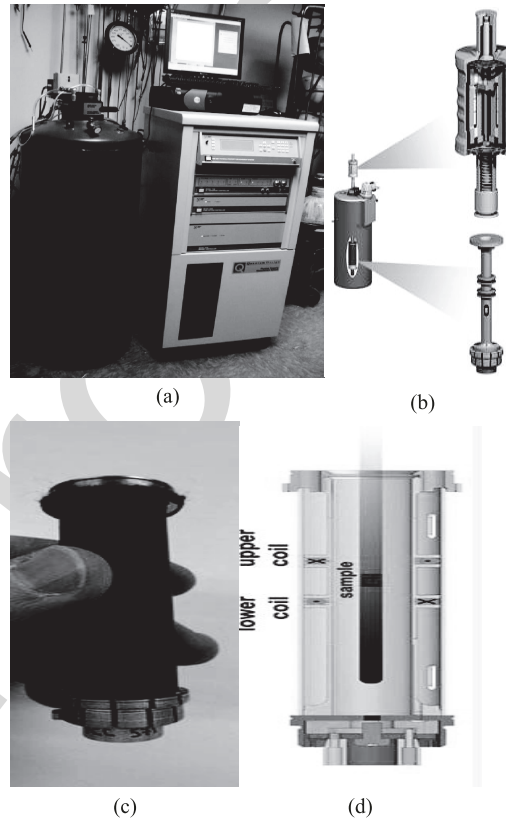


Fig. 2. (a) PPMS apparatus. (b) VSM attachments for PPMS. (c) Photograph of the VSM puck. (d) Cross section of VSM puck.

A physical property measurement system (PPMS) with VSM attachments [Fig. 2(a) and (b)] was used to measure the magnetic moment in the NiFeO sample prepared at the AJA sputtering system in the clean room of Texas State University. The PPMS system and VSM attachments are shown as follows. The pickup coils for this apparatus are in the VSM puck [Fig. 2(c) and (d)], which is inserted into the PPMS. This system may measure fields ranging from +9 to -9 T and can measure temperatures ranging from 4 to 300 K. For these measurements, the field was changed at a rate of 180 Oe/s, and measurements were done at 4 K and at room temperatures.

137 C. XPS Measurement Procedure

X-ray photoelectron spectroscopy (XPS) measurements 138 were made using an XPS PHI Quantum 2000 Scanning ESCA 139 microprobe. The XPS chamber contains an Al $\text{K}\alpha$ X-ray source 140 in which incoming X-rays are parallel to the surface normal. 141 The system allows for measurements with an analysis resolution 142 of about 1 eV [5]. The beam power was 50 W and 143

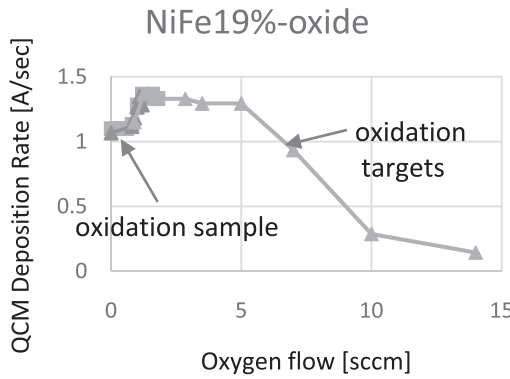


Fig. 3. Deposition rate as a function of the oxygen flow for NiFe-19% co-sputtering at 200 W.

144 the takeoff angle was 45° . The X-ray spot size was $200\ \mu\text{m}$
 145 and the analysis was done on an area of $500\ \mu\text{m} \times 500\ \mu\text{m}$. Under these conditions, the information depth is approximately
 146 10 nm. Prior to the scans, part of the Pt or Au cap layer
 147 was removed by argon sputtering. To avoid the effects of
 148 preferential sputtering on the NiFe-oxide XPS spectra, part of
 149 the cap layers were kept in place. As Au has a larger sputter
 150 rate, the samples with an Au cap layer were sputtered for only
 151 1 min while the samples covered with a Pt cap layer were
 152 sputtered for 3 min. The pass energies were 187 eV for the
 153 survey and 58 eV for the high-resolution scans. All energies
 154 are referenced with respect to the main C peak at 284.8 eV.
 155

156 III. EXPERIMENTAL RESULTS

157 Fig. 3 shows the measured deposition rate as a function
 158 of the oxygen flow for our process. The deposition shows a
 159 maximum as the function of the oxygen flow. At lower oxygen
 160 flow rates, the deposition rate increases with the oxygen flow.
 161 We believe that this increase (24%) is due to the introduction
 162 of oxygen into the system resulting in the oxidation of the
 163 freshly deposited film. As for a fully oxidized film one would
 164 expect an increase in 27%, the films sputtered at low oxygen
 165 flow are not stoichiometric but contain a significant amount
 166 of oxygen vacancies. At higher oxygen flow, i.e., above
 167 5 sccm, the deposition rate decreases strongly. We believe
 168 that this is caused by the oxidation of the targets. This is
 169 often referred to as poisoning of the target [8]. It is well
 170 known that NiFe-oxide has a much lower sputter rate than
 171 metallic permalloy. Although the oxidation of the targets also
 172 takes place at lower oxygen flow rates, at those low oxygen
 173 flow rates, the removal rate of the material from the targets
 174 is much higher than the rate with which an oxide layer is
 175 formed on the target. Therefore, below 5 sccm, the target
 176 surfaces are clean of oxide and most of the sputtered material
 177 is metallic permalloy. From 5 sccm and above, the removal
 178 of the material from the targets can no longer keep up with
 179 the oxidation and the deposition rate collapses. Note that for
 180 our process, the QCM deposition rate is significantly lower
 181 than the rate with which the material is removed from the
 182 targets. The short mean free path of the sputtered atoms at
 183 8 mtorr results in a diverging atom beam that has a diameter
 184 significantly larger than the target diameter at the location

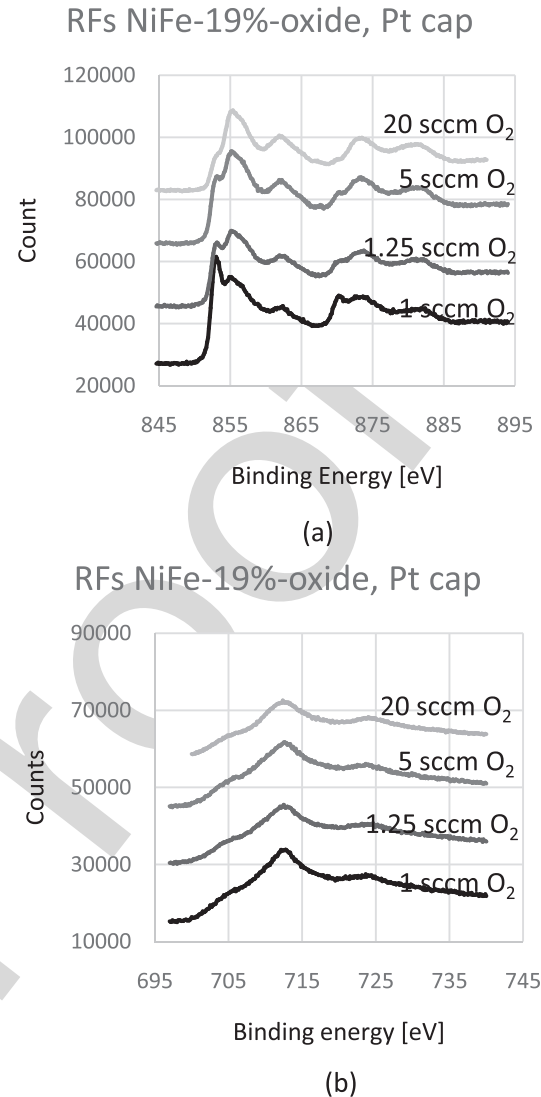


Fig. 4. XPS spectra of RF-sputtered NiFe-oxide samples sputtered at different oxygen flow rates covered with the Pt cap layer. (a) Ni spectrum. (b) Fe spectrum. Spectra are shifted in the y-direction to reveal the detail.

185 of the substrate. From the measurements of the deposition
 186 rate versus the substrate distance, we expect at least a factor
 187 10 difference between the QCM rate at our substrate position
 188 and the target material removal rate. Fig. 4 shows the XPS
 189 spectrum of $\text{Ni}(2p_{3/2})$ and $\text{Fe}(2p)$ of samples sputtered at
 190 various oxygen flow rates. This is the XPS data obtained from
 191 the samples that had a Pt cap layer. Note that the ratio of the
 192 Ni^0 to Ni^{2+} decreases with oxygen flow, but the Ni^0 peak is
 193 still visible in the Ni-spectrum for films sputtered at 20 sccm
 194 oxygen flow. The Fe-XPS spectra of the films sputtered at
 195 a different oxygen flow look very similar to each other
 196 (see Fig. 4). Our Fe spectra differ though from the XPS spectra
 197 of oxidized Permalloy films published in [9], which show a
 198 steep slope at 700 eV while all our films show a very gradual
 199 slope. The absence of a distinct Fe^0 peak suggests that most
 200 Fe is oxidized, and oxygen vacancies prefer to reside next
 201 to nickel atoms. Since the resistivity of the films sputtered at
 202 20 sccm O_2 is much lower than the films sputtered at 5 sccm, we
 203 believe that the films sputtered at 20 sccm oxygen

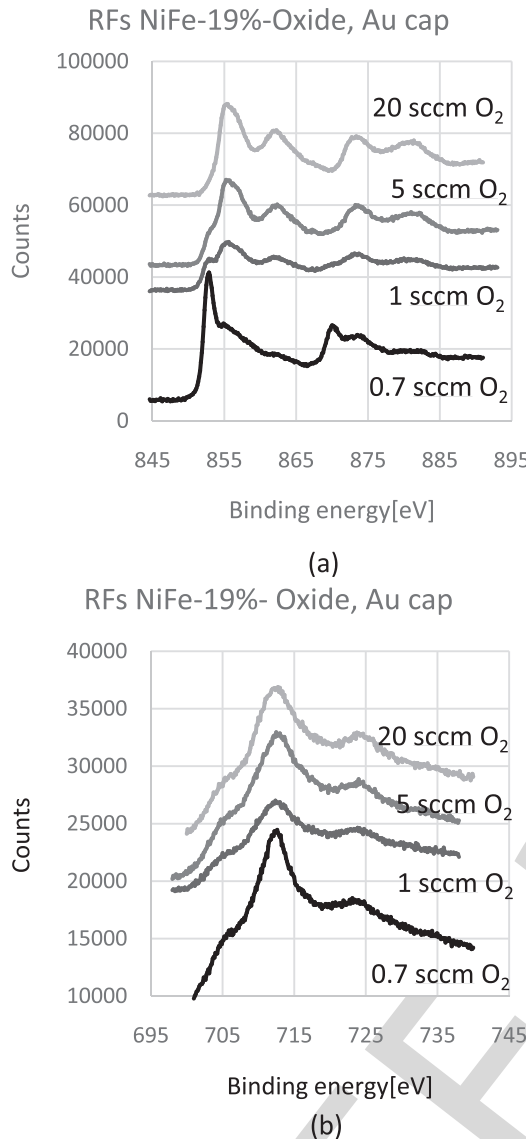


Fig. 5. XPS spectra of RF-sputtered NiFe-oxide samples sputtered at different oxygen flow rates covered with the Au cap layer. (a) Ni spectrum. (b) Fe spectrum. Spectra are shifted in the y-direction to reveal the detail.

flow contain metal vacancies. However, no Ni^{3+} peak was observed in our NiFe-oxide films [10]. The interpretation of the Fe-XPS spectrum is challenging as for Al $\kappa\alpha$ radiation an Auger Ni-peak is present in the middle of the Fe-XPS spectrum, i.e., 712 eV. In addition, Pt has a peak in the Fe-XPS spectrum at 725 eV near the position of a metallic Fe peak. The XPS data for the samples covered with an Au cap layer are shown in Fig. 5. Note that the counts of the Au-capped samples of Fig. 5 are significantly lower than those of the Pt capped layers of Fig. 4. This suggests that the remaining Au cap layer in the samples of Fig. 5 is thicker than the remaining Pt cap layer in the samples of Fig. 4. A detailed analysis of the data of Figs. 4 and 5 using a rough estimate of the sputter rates of Au and Pt suggests that we might have sputtered through part of the Pt layer for the results shown in Fig. 4 and that the ratio of the Ni^0 to Ni^{2+} oxygen peaks in Fig. 4 was affected by a preferential sputtering of oxygen of part of the NiFeO films of Fig. 4. The Fe spectra of Fig. 5 are similar to the

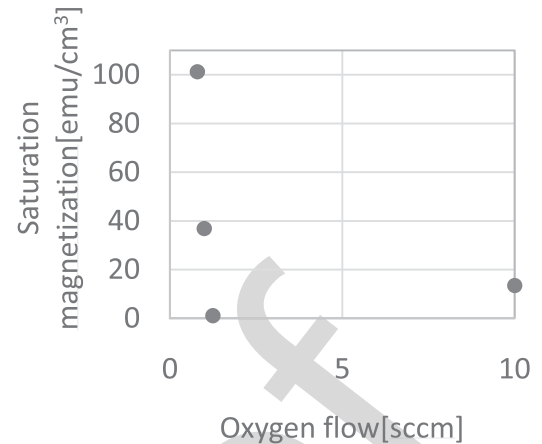


Fig. 6. Variation of saturation magnetization with oxygen concentration for different films.

Fe spectra of Fig. 4. It might not be possible to distinguish the metallic Fe-XPS peak at 707 eV from the Ni Auger peak at 712 eV. An additional XPS analysis was done in another system using Mg $\kappa\alpha$ radiation on uncapped layers. For an Mg source, the nickel Auger peaks shift outside the Fe spectrum. The same gradual slope in the XPS Fe spectrum near 700 eV was observed for those experiments. Therefore, the gradual slope observed in the Fe spectrum might be characteristic for reactive RF-sputtered PyO films. It is definitely not caused by the cap layer and does not depend on the X-ray source, so is unlikely due to the Auger peak of nickel.

Fig. 6 shows the measured magnetic moment per unit volume as a function of the oxygen flow. A decrease in the saturation magnetization is observed for higher oxygen flows. This might be due to a more fully oxidation of the films sputtered at high oxygen flow. Note that NiFe-oxide was shown to have a rock salt crystal structure [11], [12] and discrete Fourier transform calculations have shown that it is antiferromagnetic [13]. A sharp decrease in the magnetic moment was observed when the oxygen flow was increased to 1.25 sccm. For films deposited at flows above 1.25 sccm, the saturation magnetization slightly increases similar to what was observed by Twagirayezu on RF-sputtered films using a single source [2].

IV. CONCLUSION

The deposition rate of reactive RF-sputtered NiFeO and NiO films depends on the oxygen flow rate during deposition. For low oxygen flows (below 1.25 sccm O_2), the deposition rate increases with increased oxygen flow. This is caused by the oxidation of the deposited metal film. This is consistent by magnetic measurements that show an increase in the magnetic moment for films sputtered at lower O_2 flows. At moderate oxygen flows, i.e., between 1.25 and 5 sccm, the deposition rate is constant. At high oxygen flow (above 5 sccm), the deposition rate sharply decreases. At these flows, the sputtering of the material of the target can no longer keep up with its oxidation and poisoning of the target takes place. The XPS analysis showed that the ratio of the Ni^0 to Ni^{2+} decreases with oxygen flow. The XPS results also

suggest that sputtering NiFe-oxide with argon leads to the preferential sputtering of oxygen (a reduction of NiFeO) for oxygen-rich compositions. The XPS Fe spectra of the films sputtered at a different oxygen flow look very similar to each other but different from Fe-XPS spectra measured on oxidized permalloy samples by others. A distinct metallic Fe peak was lacking in the Fe spectra, which suggests that oxygen vacancies in NiFe-oxide prefer nickel neighbors and most of the Fe atoms are oxidized. The observed increase in the magnetic moment with oxygen vacancy concentration could provide a method to magnetically detect the location and distribution of low oxygen concentration filaments in RRAM devices. Such method is in need of systematic switching studies to further the development of the RRAM technology.

ACKNOWLEDGMENT

This work was supported in part by a DOD Grant (HBCU/MI) under Grant W911NF-15-1-0394 and in part by NSF through a DMR-MRI Grant under Award 1726970. The authors would like to thank the staff of the nanofabrication fab at Texas State for their support, particularly A. Sherrow and Dr. C. Smith. They would also like to thank Dr. T. Hossain and A. Ghatak-Roy for their help with the XPS measurements.

REFERENCES

- [1] I. Hotovy, J. Huran, L. Spiess, S. Hascik, and V. Rehacek, "Preparation of nickel oxide thin films for gas sensors applications," *Sens. Actuators B, Chem.*, vol. 57, pp. 147–152, Sep. 1999.
- [2] F. Twagirayezu, M. A. AhadTalukder, and W. J. Geerts, "Magnetic properties of RF sputtered NiO and Ni_{0.8}Fe_{0.2}O₁-samples grown on SiO₂/Si substrates," *Mater. Res. Innov.*, Jul. 2018.
- [3] AJA International Incorporated. [Online]. Available: <http://www.ajaint.com/atac-orion-series>
- [4] J. Hack, M. H. Ludwig, W. Geerts, and R. E. Hummel, "Advances in micro-crystalline and nano-crystalline semiconductors," vol. 452, p. 147, 1997.
- [5] E. O. Samwel, T. Bolhuis, and J. C. Lodder, "An alternative approach to vector vibrating sample magnetometer detection coil setup," *Rev. Sci. Instrum.*, vol. 69, no. 9, p. 3204, 1998.
- [6] S. Thota, J. H. Shim, and M. S. Seehra, "Size-dependent shifts of the Néel temperature and optical band-gap in NiO nanoparticles," *J. Appl. Phys.*, vol. 114, no. 21, p. 214307, 2013.
- [7] C. D. Wanger *et al.*, *Handbook of X-Ray Photoelectron Spectroscopy*. 1997.
- [8] N. R. Murphy, L. Sun, J. T. Grant, J. G. Jones, and R. Jakubiak, "Molybdenum oxides deposited by modulated pulse power magnetron sputtering: Stoichiometry as a function of process parameters," *J. Electron. Mater.*, vol. 44, pp. 3677–3686, Oct. 2015.
- [9] M. Salou, B. Lescop, S. Rioual, A. Lebon, J. Ben Youssef, and B. Rouvelliou, "Initial oxidation of polycrystalline Permalloy surface," *Surf. Sci.*, vol. 602, pp. 2901–2906, Sep. 2008.
- [10] S. Uhlenbrock, C. Scharfschwerdt, M. Neumann, G. Illing, and H.-J. Freund, "The influence of defects on the Ni₂p and O 1s XPS of NiO," *J. Phys., Condens. Matter*, vol. 4, no. 40, pp. 7973–7978, 1992.
- [11] M. A. A. Talukder, Y. Cui, M. Compton, W. Geerts, L. Scolfaro, and S. Zollner, "FTIR ellipsometry study on RF sputtered permalloy-oxide thin films," *MRS Adv.*, vol. 1, no. 49, pp. 3361–3366, 2016.
- [12] A. K. Bandyopadhyay, S. E. Rios, A. Tijerina, and C. J. Gutierrez, "The influence of ion beam sputtering geometry on metastable (Ni₈₁Fe₁₉)O/Ni₈₁Fe₁₉ exchange biased bilayers," *J. Alloys Compounds*, vol. 369, pp. 217–221, Apr. 2004.
- [13] J. E. Petersen, F. Twagirayezu, L. M. Scolfaro, P. D. Borges, and W. J. Geerts, "Electronic and optical properties of antiferromagnetic iron doped NiO—A first principles study," *AIP Adv.*, vol. 7, no. 5, p. 055711, 2017.

AUTHOR QUERIES

AUTHOR PLEASE ANSWER ALL QUERIES

PLEASE NOTE: We cannot accept new source files as corrections for your paper. If possible, please annotate the PDF proof we have sent you with your corrections and upload it via the Author Gateway. Alternatively, you may send us your corrections in list format. You may also upload revised graphics via the Author Gateway.

AQ:1 = Please confirm whether the author name “Binod D. C.” is correct as set.

AQ:2 = Please provide expansions for MSEC, AJA, MKS, and ESCA.

AQ:3 = Please provide in-text citations for Fig. 1.

AQ:4 = Please check and confirm whether the citation for Fig. 2 provided in the sentence “A physical property measurement system (PPMS)...” is correct.

AQ:5 = Author: Please confirm or add details for any funding or financial support for the research of this article.

AQ:6 = Please confirm author names, article title, and journal title for ref. [2]. Also provide the volume no., and page range.

AQ:7 = Please provide the accessed date for ref. [3].

AQ:8 = Please confirm the author names, and title for ref. [4]. Also provide the journal title.

AQ:9 = Please provide the publisher name and publisher location for ref. [7].